Journal of Chromatography, 594 (1992) 1–8
Elsevier Science Publishers B.V., Amsterdam

CHROM. 23 889

Improved equations for the calculation of chromatographic figures of merit for ideal and skewed chromatographic peaks

Mark S. Jeansonne[☆] and Joe P. Foley*,[☆☆]

Department of Chemistry, Louisiana State University, Baton Rouge, LA 70803-1804 (USA)

(Received July 24th, 1991)

ABSTRACT

Improved empirical equations based on the graphically measurable parameters peak height (h_p), width (W) and asymmetry (b/a) at 10, 25, 50, 71, 73, 75, 77 and 79% of the peak height have been derived. These equations were developed using the exponentially modified Gaussian function as an asymmetric peak model. Equations are reported for the following chromatographic figures of merit: τ, σ_G, area, variance, third and fourth statistical moments, excess, and skew. The accuracy and precision of the equations are discussed, along with their applicability to fronted and overlapped peaks.

INTRODUCTION

In a recent publication we presented an equation-based approach for the accurate measurement of chromatographic peak statistical moments, excess, and skew [1]. These empirical equations, based on the exponentially modified Gaussian (EMG) function, utilize the peak width, asymmetry, and in some cases, the peak height. The EMG function, resulting from the convolution of Gaussian and exponential decay functions, can model any tailed peak more accurately than a Gaussian function. Due to various intra and extracolumn band broadening process, real chromatographic peaks are seldom symmetrical, so that use of a tailed peak model should be more accurate. The EMG function has been justified both theoretically [2–4] and experimentally [5,6] and has been thoroughly reviewed [7,8]. Because a convenient procedure for verification of the EMG character of chromatographic peaks exists [5], these equations can be confidently applied once EMG peak shape has been established.

A variety of approaches have been used to make this model more practical for routine use [5,9–16]. One particularly popular approach has been to relate the graphical parameters a and b, (see Fig. 1), measured at a particular fraction of the peak height, to the fundamental EMG parameters, τ and σ_G. Relationships between a and b and the EMG parameters have been reported in the form of both graphical curves and empirical equations. Both techniques circumvent tedious, computer intensive curve fitting. Equations reported by Foley and Dorsey [11] in 1983 have perhaps shown the greatest routine applicability, based on the number of citations. In that work, equations were derived for the calculation of many important chromatographic peak parameters (*i.e.*, τ, σ_G, statistical moments and efficiency) that were collectively termed chromatographic figures of merit (CFOMs). Equations based on the measurement of b and a at 10, 30 and 50% of the peak height fraction were reported, although

☆ Present address: Chevron Chemical Co., 1862 Kingwood Drive, Kingwood, TX 77339, USA.
☆☆ Present address: Department of Chemistry, Villanova University, Villanova, PA 19085-1699, USA.

0021-9673/92/$05.00

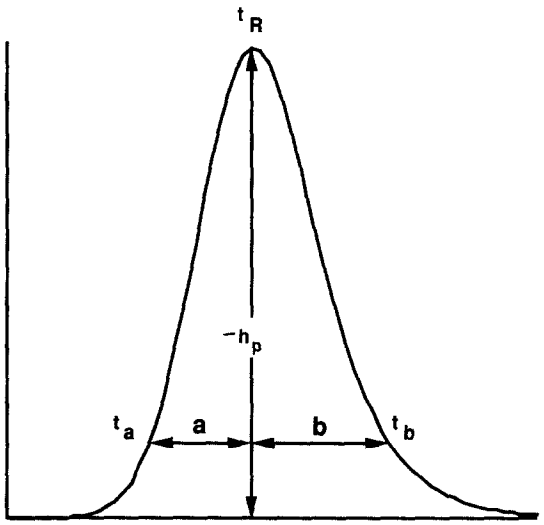

Fig. 1. Graphical parameters necessary for calculation of various chromatographic figures of merit (CFOMs). h_p = Peak height; $W = a + b$ = peak width; (b/a) = peak asymmetry.

only the equations at 10% were recommended for calculation of the CFOMs. The equations at 30 and 50% were intended solely for peak modeling.

Although the CFOM equations reported by Foley and Dorsey earlier are very accurate and precise, they were intended to be used with manually measured b and a values where the accuracy of these measurements was the limiting factor in the accuracy of the equations. Due to the greater accuracy of graphical parameter measurement via modern electronic integrators and data systems, the accuracy of CFOM measurement may be unnecessarily limited by the equations themselves. Two additional limitations are (i) the somewhat narrow asymmetry (b/a) range of the equations; and (ii) the absence of equations based on peak measurements higher than 50% of the peak height.

With regard to (ii), the ability to use b and a from higher peak height fractions is desirable when peaks are overlapped because distortion from the adjacent peak is less. We have shown that accurate measurement of CFOMs utilizing b and a measurements at 75% of the peak height is possible for both overlapping and resolved peaks using improved equations that we did not specify [1]. In this paper we report those improved equations (from the standpoint of the previous limitations) for the measurement of peak area, variance (M_2), third (M_3) and fourth (M_4) statistical moments, excess, and skew.

EXPERIMENTAL

An Apple Macintosh Plus microcomputer programmed in Microsoft Basic was used for EMG peak generation. The EMG function was evaluated as described before [5], and universal data were obtained via a search algorithm [7]. All polynomial curve fitting was done using commercially available software.

EMG peak generation

Eqn. 1 shows the form of the EMG function used.

$$h_{EMG}(t) = \frac{A}{\tau}\exp\left[\frac{1}{2}\left(\frac{\sigma_G}{\tau}\right)^2 - \left(\frac{t - t_G}{\tau}\right)\right] \cdot \int_{-\infty}^{z} \frac{\exp\left(\frac{-y^2}{2}\right)}{\sqrt{2\pi}}\,dy \quad (1)$$

A is the peak amplitude, τ is the exponential modifier, σ_G is the standard deviation of the unmodified Gaussian, t_G is the retention time of the unmodified Gaussian and $z = (t - t_G)/\sigma_G - \sigma_G/\tau$. The ratio τ/σ_G is used to describe the overall shape of an EMG peak; at τ/σ_G close to zero, the peak approaches Gaussian shape, while higher τ/σ_G values give greater tailing. Values of $A = 1$, $t_G = 100$ and $\sigma_G = 5$ were used for evaluation of the function. The times for t_R (EMG peak apex), t_a, and t_b were measured to within 0.001 at r (peak height fraction) = 0.10, 0.25, 0.5, 0.71, 0.73, 0.75, 0.77, and 0.79 (see Fig. 1), from $\tau/\sigma_G = 0$ to 4.5 in 0.05 increments. The peak height (h_p) at each τ/σ_G was determined concurrently with t_R using the same search algorithm. Once t_R, t_a and t_b were measured, the parameters a, b, W ($= a + b$), and asymmetry (b/a) were then calculated. Finally, the values of asymmetry (b/a), W/σ_G, $(t_R - t_G)/\sigma_G$ and h_p, termed universal data, were used in the following derivations.

Method of derivation

A three stage approach was employed for CFOM calculation: (i) derivation of width and asymmetry based equations for σ_G and M_2; (ii) calculation of τ via eqn. 2; and (iii) computation via eqns. 3–6 below of the remaining moments, excess, and skew [11].

$$\tau = \sqrt{M_2 - \sigma_G^2} \quad (2)$$

$$M_3 = 2\tau^3 \tag{3}$$

$$M_4 = 3\sigma^4 + 6\sigma^2\tau^2 + 9\tau^4 \tag{4}$$

$$\text{Skew} = \frac{M_3}{M_2^{3/2}} \tag{5}$$

$$\text{Excess} = \frac{M_4}{M_2^2} - 3 \tag{6}$$

We found that the above approach, utilizing equations for σ_G and M_2 and then eqns. 2–6 above, to be somewhat more accurate than an alternative approach based on equations for σ_G and τ/σ_G, the calculation τ from their product, and calculation of the remaining CFOMs via eqns. 3–6. Because of the poorer accuracy of the latter approach, it is not discussed further. Equations based on the first, more accurate approach were derived at several peak heights, with those for $0.71 \leqslant r \leqslant 0.79$ developed for purposes of averaging to reduce uncertainty and bias.

Derivation of equations for σ_G

At each relative peak height (r), the quantity W_r/σ_G was plotted as a function of asymmetry (b/a), giving results similar to Fig. 2 for $r = 0.25$. As shown, the plot is curved at the lower b/a values and linear at the higher values. Therefore, a quadratic least-squares fit was used at lower asymmetries and a linear least-squares fit was used for higher asymmetries, resulting in two (nonoverlapping) equations at each r. σ_G could then be related to width and asymmetry as shown in eqn. 7.

$$\sigma_G = \frac{W_r}{\text{f}(b/a)} \tag{7}$$

where f(b/a) is the resulting fitted equation of the form $\text{f}(b/a) = C_0 + C_1(b/a) + C_2(b/a)^2$ [The coefficient C_2 is 0 for f(b/a) resulting from the linear fit.] Table I lists the coefficients obtained at each r for both linear and quadratic fits and their valid asymmetry ranges. The cut point between curved and linear fits was determined so that the relative error in σ_G over the entire b/a range was minimized.

Derivation of equations for M_2

Analogous to the derivations of σ_G equations, the quantity M_2/W_r^2 was plotted *vs.* asymmetry (b/a) at each r. However, as shown in Fig. 3 for $r = 0.25$, curvature was evident over the entire b/a range.

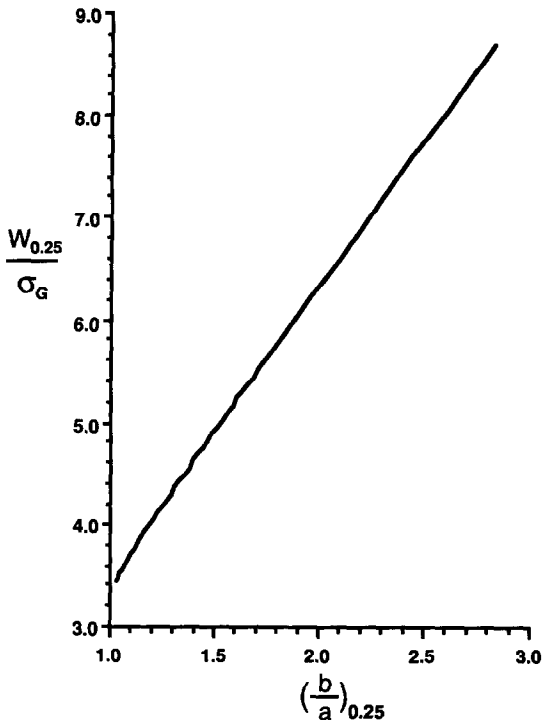

Fig. 2. Determination of f(b/a) for σ_G at $r = 0.25$. Note slight curvature at lower asymmetries. Quadratic fit from $(b/a)_{0.25} = 1.02$ to 1.26, linear fit from $(b/a)_{0.25} = 1.26$ to 2.85.

Moreover, because an accurate quadratic fit over the entire b/a range was not possible, two separate least-squares quadratic fits were used, again choosing the cut point to minimize the relative error over the entire asymmetry range. Eqn. 8 shows the resulting relationship between M_2, W_r^2 and f(b/a).

$$M_2 = W_r^2 \cdot \text{f}(b/a) \tag{8}$$

Values of the coefficients of f(b/a) for calculation of M_2 are also given in Table I. At r values of 0.71 to 0.79, the plots were similar to those obtained for the σ_G derivations, thereby allowing linear and quadratic fits for the two sections of curves, as before.

Calculation of remaining CFOMs except peak area

Using calculated values of σ_G and M_2 (equations of Table I), values for τ, M_3, M_4, skew, and excess were calculated at $r = 0.10$, 0.25, 0.5, 0.71, 0.73, 0.75, 0.77, and 0.79 via eqns. 2–6, from $\tau/\sigma_G = 0$ to 4.5 in increments of 0.05. The accuracy and precision of these values is reported in Table II.

TABLE I

COEFFICIENTS, ACCURACY, AND PRECISION OF EQUATIONS FOR CALCULATING σ_G AND M_2 OF GAUSSIAN AND EMG PEAKS

Parameter[a]	Peak height fraction, r	Asymmetry range, τ/σ	Asymmetry range, $(b/a)_r$	Coefficients[b]			Maximum error[c] (%)	Relative uncertainty[d] (%)
				C_2	C_1	C_0		
σ_G	0.10	0.30–1.20	1.03–1.46	−1.2951	6.6162	−0.9516	−0.2, +0.6	±0.52
		1.20–4.30	1.46–3.67	0	3.3139	1.1147		
	0.135	0.30–0.65	1.02–1.14	−4.1347	12.7655	−4.5742	−0.2, +0.3	±0.53
		0.65–4.30	1.14–3.42	0	3.1665	1.0051		
	0.25	0.30–1.10	1.02–1.26	−2.4352	8.8715	−3.0485	±0.2	±0.52
		1.10–4.30	1.26–2.85	0	2.8504	0.6888		
	0.50	0.30–1.30	1.01–1.21	−4.2670	12.5178	−5.8561	−0.4, +0.8	±0.8
		1.30–4.30	1.21–2.09	0	2.4685	0.0981		
	0.71	0.30–1.85	1.01–1.23	−2.7901	9.0992	−4.6165	−0.5, +0.2	±1.0
		1.85–4.30	1.23–1.64	0	2.2527	−0.3983		
	0.73	1.30–1.85	1.01–1.22	−2.9116	9.3374	−4.8028	−0.5, +0.2	±1.0
		1.85–4.30	1.22–1.60	0	2.2449	−0.4666		
	0.75	0.30–1.25	1.01–1.12	−7.4174	18.8306	−9.8710	±0.7	±1.2
		1.30–4.30	1.12–1.56	0	2.3245	−0.6604		
	0.77	0.30–1.85	1.01–1.19	−3.3185	10.1672	−5.3703	−0.5, +0.2	±1.1
		1.85–4.30	1.19–1.52	0	2.2326	−0.6111		
	0.79	0.30–1.90	1.01–1.19	−3.3724	10.2546	−5.4779	−0.5, +0.2	±1.2
		1.90–4.30	1.19–1.49	0	2.2268	−0.6859		
M_2	0.10	0.30–1.15	1.03–1.46	0.1270	−0.06458	0.4766	−0.2, +0.6	±0.6
		1.15–4.30	1.46–3.67	−0.0299	0.3569	0.1909		
	0.135	0.30–2.85	1.03–2.50	−0.0378	0.4993	0.1470	−1.4, +0.5	±0.6
		2.85–4.30	2.50–3.42	0	0.2493	0.5394		
	0.25	0.30–0.70	1.02–1.13	2.3418	−4.1376	2.6930	−0.2, +0.3	±0.8
		0.70–4.30	1.13–2.85	−0.1842	1.6032	−0.5715		
	0.50	0.30–1.30	1.01–1.21	7.9161	−12.8196	6.6750	−0.6, +0.4	±1.5
		1.30–4.30	1.21–2.09	−1.3369	9.3616	−6.6407		
	0.71	0.30–1.30	1.01–1.14	52.777	−96.293	47.101	−0.6, +0.8	±2.4
		1.30–4.30	1.14–1.64	0	25.039	−22.696		
	0.73	0.30–1.35	1.01–1.14	63.545	−116.389	56.743	−1.0, +0.5	±2.6
		1.35–4.30	1.14–1.60	0	29.935	−27.601		
	0.75	0.30–1.40	1.01–1.13	84.448	−157.205	77.0333	−1.3, +0.7	±2.8
		1.40–4.30	1.13–1.56	0	35.9111	−33.5484		
	0.77	0.30–1.70	1.01–1.17	79.771	−142.903	67.779	−1.3, +0.7	±2.7
		1.70–4.30	1.17–1.52	0	44.119	−41.993		
	0.79	0.30–1.70	1.01–1.16	103.956	−188.641	89.840	−1.3, +0.7	±2.9
		1.70–4.30	1.16–1.49	0	54.353	−52.398		

[a] General form of the equations for each parameter: $\sigma_G = W_r/f(b/a)$; and $M_2 = W_r^2 \cdot f(b/a)$, where W_r = width of peak at the peak height fraction given by the subscript, b/a = an asymmetry factor measured at the same peak height fraction as the width, and $f(b/a) = C_0 + C_1(b/a) + C_2(b/a)^2$.

[b] Tabulated values multiplied × 10 for M_2.

[c] Maximum relative error of the equations over the stated asymmetry range.

[d] Percent relative standard deviation (%R.S.D.) predicted from error propagation, assuming R.S.D. values of 0.25% and 0.5% for W_r and b/a. Note that the precision of W and b/a can be better than what we have assumed for many data acquisition systems. In instances where a range is reported, the larger number refers to the least asymmetric peak (smallest b/a value) and the smaller number refers to the most asymmetric peak (largest b/a value). The uncertainty decreases *exponentially* from the larger value to the lower value as b/a increases.

TABLE II

ERROR AND UNCERTAINTY OF CFOMs CALCULATED FROM σ_G AND M_2 USING EQNS. 2–6 (TEXT)[a]

Parameter	Peak height fraction, r	Asymmetry range, τ/σ	Asymmetry range, $(b/a)_r$	Maximum error (%)	Relative uncertainty (%)
τ (eqn. 2, text)	0.10	0.5–4.3	1.09–3.67	−0.4, +0.2	2.4–0.3
	0.135	0.5–4.3	1.08–3.42	−0.3, +0.7	2.6–0.3
	0.25	0.5–4.3	1.07–2.85	±0.4	3.0–0.3
	0.50	0.5–4.3	1.04–2.09	−0.4, +0.6	4.2–0.4
	0.71	0.5–4.3	1.03–1.64	−0,4, +0.6	5.8–0.6
	0.73	0.5–4.3	1.03–1.60	−0.7, +0.4	6.1–0.7
	0.75	0.5–4.3	1.03–1.56	±0.8	6.5–0.7
	0.77	0.5–4.3	1.02–1.52	−0.5, +1.0	7.0–0.8
	0.79	0.5–4.3	1.02–1.49	−0.8, +1.0	7.3–0.8
τ/σ	0.10	0.5–4.3	1.09–3.67	−0.8, +0.3	2.5–0.6
	0.135	0.5–4.3	1.08–3.42	−0.3, +0.8	2.7–0.6
	0.25	0.5–4.3	1.07–2.85	±0.5	3.0–0.6
	0.50	0.5–4.3	1.04–2.09	−1.0, +0.6	4.3–0.7
	0.71	0.5–4.3	1.03–1.64	−0.6, +0.9	5.9–0.9
	0.73	0.5–4.3	1.03–1.60	−0.6, +0.9	6.2–0.9
	0.75	0.5–4.3	1.03–1.56	−0.9, +1.4	6.6–1.0
	0.77	0.5–4.3	1.02–1.52	−0.6, +0.9	7.1–1.0
	0.79	0.5–4.3	1.02–1.49	±0.8	7.4–1.1
M_3 (eqn. 3, text)	0.10	0.5–4.3	1.09–3.67	−1.0, +0.5	7.3–0.9
	0.135	0.5–4.3	1.08–3.42	−0.9, +2.2	7.8–0.9
	0.25	0.5–4.3	1.07–2.85	−1.2, +1.1	8.8–0.9
	0.50	0.5–4.3	1.04–2.09	−1.2, +1.9	12.6–1.2
	0.71	0.5–4.3	1.03–1.64	−1.1, +1.7	17.5–2.0
	0.73	0.5–4.3	1.03–1.60	−2.0, +1.4	18.3–2.0
	0.75	0.5–4.3	1.03–1.56	−2.4, +2.5	19.6–2.1
	0.77	0.5–4.3	1.02–1.52	−1.5, +2.9	20.9–2.3
	0.79	0.5–4.3	1.02–1.49	−2.5, +2.9	22.0–2.4
M_4 (eqn. 4, text)	0.10	0.5–4.3	1.09–3.67	−0.6, +0.9	3.1–1.2
	0.135	0.5–4.3	1.08–3.42	−0.5, +1.2	3.1–1.2
	0.25	0.5–4.3	1.07–2.85	−0.5, +0.9	3.5–1.2
	0.50	0.5–4.3	1.04–2.09	±0.9	4.9–1.6
	0.71	0.5–4.3	1.03–1.64	−1.2, +1.6	6.7–2.6
	0.73	0.5–4.3	1.03–1.60	−2.3, +1.4	7.0–2.7
	0.75	0.5–4.3	1.03–1.56	−2.8, +2.3	7.6–2.8
	0.77	0.5–4.3	1.02–1.52	−1.7, +1.6	8.0–3.0
	0.79	0.5–4.3	1.02–1.49	−2.9, +1.7	8.4–3.2
Skew (eqn. 5, text)	0.10	0.5–4.3	1.09–3.67	−1.0, +0.6	7.3–1.2
	0.135	0.5–4.3	1.08–3.42	−0.7, +1.5	7.9–1.3
	0.25	0.5–4.3	1.07–2.85	−1.2, +0.9	8.9–1.3
	0.50	0.5–4.3	1.04–2.09	−1.2, +1.3	12.7–1.6
	0.71	0.5–4.3	1.03–1.64	−1.0, +1.1	17.7–2.7
	0.73	0.5–4.3	1.03–1.60	−1.1, +0.7	18.5–2.8
	0.75	0.5–4.3	1.03–1.56	−2.3, +1.8	19.8–3.0
	0.77	0.5–4.3	1.02–1.52	−0.4, +2.1	21.2–3.1
	0.79	0.5–4.3	1.02–1.49	−0.9, +1.8	22.2–3.3
Excess (eqn. 6, text)	0.10	0.5–4.3	1.09–3.67	−1.3, +0.8	42.1–2.5
	0.135	0.5–4.3	1.08–3.42	−0.9, +2.0	45.4–2.6
	0.25	0.5–4.3	1.07–2.85	−1.6, +1.2	51.1–2.7
	0.50	0.5–4.3	1.04–2.09	−1.6, +1.8	73.0–3.4
	0.71	0.5–4.3	1.03–1.64	±1.4	102–5.5

(*Continued on p. 6*)

TABLE II (*continued*)

Parameter	Peak height fraction, r	Asymmetry range, τ/σ	Asymmetry range, $(b/a)_r$	Maximum error (%)	Relative uncertainty (%)
Excess (eqn. 6, text)	0.73	0.5–4.3	1.03–1.60	−1.4, +0.9	106–5.8
	0.75	0.5–4.3	1.03–1.56	−3.0, +2.5	105–6.1
	0.77	0.5–4.3	1.02–1.52	−0.6, +2.8	122–6.4
	0.79	0.5–4.3	1.02–1.49	−1.2, +2.5	128–6.8

[a] Refer to Table I for an explanation of terms.

Derivation of area equations

Area equations based on width, asymmetry, and peak height measurements at $r = 0.10$, 0.25, 0.50, and 0.75 have been previously reported [5] along with the method of their derivation. Additional area equations at $r = 0.71$, 0.73, 0.77, and 0.79, were derived in this report for purposes of comparison. The area equations for these r values are reported in Table III along with the area equations at $r = 0.10$, 0.25, 0.50, and 0.75 previously reported [5].

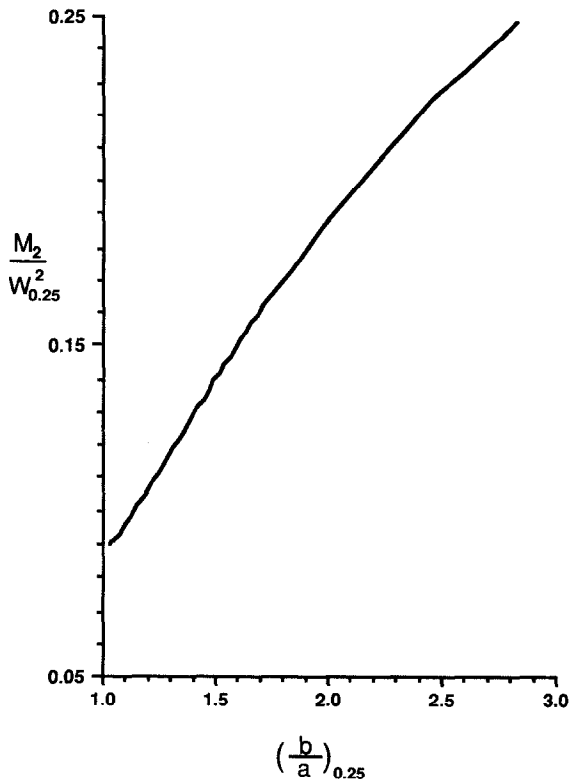

Fig. 3. Determination of f(b/a) for M_2 at $r = 0.25$. Note moderate curvature over entire asymmetry range. First quadratic fit from $(b/a)_{0.25} = 1.02$ to 1.13, second quadratic fit from $(b/a)_{0.25} = 1.13$ to 2.85.

RESULTS AND DISCUSSION

Accuracy of CFOM equations

Tables I and II show the maximum errors over the τ/σ_G range 0.3 to 4.3 for the equations derived for the various CFOMs considered in this study. In general, the equations for σ_G are accurate to within 1% while those for M_2 are accurate to within 2%. Table IV compares the results of the maximum errors reported for the Foley–Dorsey [11] equations to those reported in Tables I and II. Because Anderson and Walters [13] also derived equations for M_1, M_2, σ_G, and τ, the relative errors for their equations are reported in Table IV for purposes of comparison. Only CFOMs at $r = 0.10$ are compared, because the Foley–Dorsey equations at other r values are useful only for peak modeling and should not be used for CFOM calculation. For all CFOMs considered, the accuracy of the present set of equations is better than those derived by the previous methods. Although the Anderson–Walters equations provide a greater valid asymmetry range, most experimental peaks will have asymmetries within the valid range of the present equations. Because our equations give better accuracy than the other methods while providing for the calculation of the higher moments (whereas the Anderson–Walters equations do not), they should be the method of choice in most instances. Also, our equations for higher r (not available previously) allow the calculation of CFOMs when the lower peak height fractions are not accessible due to peak overlap [1,17].

Precision of CFOM equations

Also reported in Tables I and II are the relative

TABLE III

PEAK AREA EQUATIONS FOR EMG AND GAUSSIAN PEAKS[a]

r	Equation	R.E.[b] (%)	R.S.D.[c] (%)
0.1	$A = 0.586\ h_p\ W_{0.1}\ (b/a)^{-0.133}$	±0.50	0.36
0.135	$A = 0.631\ h_p\ W_{0135}\ (b/a)^{-0.105}$	−0.3, +0.6	0.36
0.25	$A = 0.753\ h_p\ W_{0.25}$	−1.0, +0.6	0.35
0.50	$A = 1.07\ h_p\ W_{0.5}\ (b/a)^{+0.235}$	−1.2, +1.0	0.37
0.71	$A = 1.514\ h_p\ W_{0.71}\ (b/a)^{+0.591}$	−1.1, +0.6	0.46
0.73	$A = 1.58\ h_p\ W_{0.73}\ (b/a)^{+0.651}$	−0.7, +1.1	0.48
0.75	$A = 1.64\ h_p\ W_{0.75}\ (b/a)^{+0.717}$	−1.1, +0.6	0.50
0.77	$A = 1.73\ h_p\ W_{0.77}\ (b/a)^{+0.763}$	−0.9, +0.6	0.52
0.79	$A = 1.82\ h_p\ W_{0.79}\ (b/a)^{+0.835}$	−1.0, +0.4	0.55

[a] A = Area of peak, h_p = peak height, W = width of peak at designated peak height fraction, and b/a is the asymmetry factor measured at the same peak height fraction as the width. See Fig. 1.

[b] Largest relative error in area over the interval $0 \leqslant \tau/\sigma \leqslant 4.3$, expressed as a percentage.

[c] Relative uncertainty (percent relative standard deviation) of the area measurement predicted from error propagation, assuming R.S.D. values of 0.25, 0.25 and 0.5% for h_p, W and b/a. Note that for many data systems the precision of h_p, W, and b/a can be better than what we have assumed.

uncertainties of the CFOMs based on error propagation, assuming relative standard deviations (R.S.D.) of 0.25 and 0.5% for width (W) and asymmetry (b/a). Note that the actual precision of the W and b/a measurements are likely to be better with most electronic integration systems, and thus our reported uncertainties are probably overstated. As seen in Table I, the R.S.D. values for σ_G and M_2 are in general less than than 2%, and less than 1% at some r values. From Table II it is evident that the values of the higher moments, excess, and skew are slightly more imprecise. In instances where a range of uncertainty is reported, the larger number refers to the least asymmetric peak, while the smaller number refers to most asymmetric peak. In general, the uncertainty decreases *exponentially* from the larger to the lower value as the asymmetry increases.

TABLE IV

COMPARISON OF MAXIMUM ERRORS FOR A VARIETY OF CFOM EQUATIONS[a]

Parameter	This report		Foley and Dorsey [11]		Anderson and Walters [13]	
	Valid b/a range	Maximum error	Valid b/a range	Maximum error	Valid b/a range	Maximum error
σ_G	1.03–3.67	−0.2, +0.6	1.09–2.76	−1.0, +0.5	1.0–5.21	−1.3, +1.6
τ	1.09–3.67	−0.4, +0.2	1.09–2.76	−1.0, +3.5	1.0–5.21	−4.0, +0.4
τ/σ_G	1.09–3.67	−0.8, +0.3	1.09–2.76	−1.0, +4.5	[b]	[b]
M_1	[b]	[b]	1.00–2.76	±1.0	1.0–5.21	−0.2, +0.1
M_2	1.03–3.67	−0.2, +0.6	1.00–2.76	−1.5, +0.5	1.0–5.21	−0.7, +1.0
M_3	1.09–3.67	−1.0, +0.5	1.09–2.76	−2.5, +10.5	[b]	[b]
M_4	1.09–3.67	−0.6, +0.9	1.09–2.76	−3.0, +1.5	[b]	[b]
Skew	1.09–3.67	−1.0, +0.6	1.09–2.76	−1.0, +10	[b]	[b]
Excess	1.09–3.67	−1.3, +0.8	1.09–2.76	−1.5, +14	[b]	[b]

[a] Equations based on measurement at $r = 0.10$.

[b] Equations not derived for this parameter.

Accuracy and precision of area equations

The maximum errors and uncertainties for the area equations derived here, along with those reported previously, are shown in Table III. The errors at all r are well within 1.5%, and are not more than 1.0% in most cases. Assuming a relative uncertainty in h_p of 0.25%, and the same R.S.D. values for W and b/a as before, the resulting uncertainty in area for all of the equations is less than 0.6%.

Application of equations to fronted and/or overlapped peaks

We have already demonstrated the advantages of EMG-based equations for both fully resolved [5,11] and overlapping [1,17] *tailed* peaks. However, these equations, including the ones in this report, can also be used with resolved or overlapping *fronted* peaks, provided that: (i) the fronted peak(s) in question resemble(s) the mirror image of an EMG peak; (ii) the definitions of a and b are reversed before using the EMG equations; and (iii) for an overlapped pair of peaks, the equations are applied to the *second* peak instead of the first (as with *tailed* peaks). Note that with regard to (i), the same peak modeling criteria used for tailed peaks [5] can be employed, so long as (ii) is followed. With respect to (iii), the area of the first peak may be obtained by subtracting the calculated area of the second peak (via EMG-based equations) from the total peak area measured electronically.

CONCLUSIONS

It is hoped that the more accurate equations presented here will facilitate greater use of the EMG peak model within electronic integrators and data systems. Because widths and asymmetries are now commonly measured by many chromatographic data systems, incorporation of these equations into existing software should be easy, thus providing better accuracy for the desired CFOMs. Also, as we demonstrated previously [1], EMG-based equations based on graphical measurements in the upper part of a peak provide for the direct measurement of CFOMs on the less distorted peak in an overlapped pair, even when the valley exceeds 50% of its height.

ACKNOWLEDGEMENT

The authors gratefully acknowledge the partial support of this work by the Computer-Aided Chemistry Division of the Perkin-Elmer Corporation.

REFERENCES

1 M. S. Jeansonne and J. P. Foley, *J. Chromatogr.*, 461 (1989) 149–163.
2 E. Grushka, *Anal. Chem.*, 44 (1972) 1733–1738.
3 J. C. Giddings, in J. C. Giddings and R. A. Keller (Editors), *Dynamics of Chromatography*, Vol. 1, Marcel Dekker, New York, 1965, pp. 85–87.
4 J. C. Sternberg, in J. C. Giddings and R. A. Keller (Editors), *Advances in Chromatography*, Vol. 2, Marcel Dekker, New York, 1966, pp. 205–270.
5 J. P. Foley, *Anal. Chem.*, 59 (1987) 1984–1987.
6 P. J. Naish and S. Hartwell, *Chromatographia*, 26 (1988) 285–296.
7 J. P. Foley and J. G. Dorsey, *J. Chromatogr. Sci.*, 22 (1984) 40–46.
8 M. S. Jeansonne and J. P. Foley, *J. Chromatogr. Sci.*, 29 (1991) 258–266.
9 W. W. Yau, *Anal. Chem.*, 49 (1977) 395–398.
10 W. E. Barber and P. W. Carr, *Anal. Chem.*, 53 (1981) 1939–1942.
11 J. P. Foley and J. G. Dorsey, *Anal. Chem.*, 55 (1983) 730–737.
12 K. H. Jung, S. J. Yun and S. H. Kang, *Anal. Chem.*, 56 (1984) 457–462.
13 D. J. Anderson and R. R. Walters, *J. Chromatogr. Sci.*, 22 (1984) 353–359.
14 P. R. Haddad and S. Sekulic, *J. Chromatogr.*, 459 (1988) 79–90.
15 N. S. Wu and M. Hu, *Chromatographia*, 28 (1989) 415–416.
16 N. S. Wu, C. P. Cai and Y. Yang, *Chromatographia*, 30 (1990) 220–222.
17 J. P. Foley, *J. Chromatogr.*, 384 (1987) 301–313.